ELEVENTH INTERNATIONAL CONFERENCE ON INTERGRANULAR AND INTERPHASE BOUNDARIES 2004

JOURNAL OF MATERIALS SCIENCE **40** (2005) 3107–3113

Orientation-dependent surface tension functions for surface energy minimizing calculations

ELLEN J. SIEM, W. CRAIG CARTER
Department of Materials Science & Engineering, MIT, Cambridge, MA 02139-4307, USA
E-mail: esiem@mit.edu

Previous numerical methods that calculate equilibrium particle shape to study thermodynamic and kinetic processes depend on interfacial (surface) free energy functions $\gamma(\hat{n})$ that have cubic symmetry and thus produce Wulff shapes W of cubic symmetry. This work introduces a construction yielding the minimal surface energy density $\gamma^{\text{convex}}(W)$ that can be determined for *any* W. Each $\gamma(\hat{n})$ that belongs to the equivalence class $\gamma(W)$ bounded by $\gamma^{\text{convex}}(W)$ can be used in an energy-minimizing calculation that depends only on W. For practical numerical calculations, this work gives two methods taking directional distance from specified orientation minima as a parameter to produce analytic forms of $\gamma(\hat{n})$ giving W as the equilibrium shape for (an otherwise unconstrained) fixed volume. Included are several two- and three-dimensional examples that demonstrate the application and utility of the model $\gamma(\hat{n})$ functions.
© *2005 Springer Science + Business Media, Inc.*

1. Introduction

Material interfaces are defect structures that increase the free energy of a system. The increase per unit interface area is the interfacial (surface) free energy density γ that generally depends on intensive thermodynamic variables, such as temperature and chemical potential [1]. The dependence on $\hat{n}$, the inclination of the interface unit normal, when all other variables are fixed, produces interface morphologies that are predominantly composed of inclinations with the smallest γ [2].

The shapes and forces associated with particle interface and boundary particle interface structures have many important implications for material behavior. For this reason, convenient interfacial free energy models would be valuable—just as models for molar free energies of solutions are useful for prediction of phase diagrams and driving forces for diffusion [3]. A phase diagram which indicates phase as a function of composition is analogous to a Wulff shape that indicates surface inclination as a function of orientation [4].

The Wulff shape W minimizes the total interfacial free energy of an isolated particle of fixed volume [5] and is completely determined by the inclination dependence of interfacial free energy through simple geometric constructions [4, 6, 7]. Equilibrium shapes of anisotropic particles that are attached to one or more deformable interfaces are likewise determined by the $\gamma(\hat{n})$ for each interface, but no general geometric construction is known for this class of shapes [8].

Recently, we have developed a numerical method for calculating shapes and stability of anisotropic particles located at interfaces and triple junctions [9]—calculations with important implications for heterogeneous nucleation [10–12] and for pinning in boundary migration [13–15]. The numerical method depends on the identification of a suitable algebraic expression for $\gamma(\hat{n})$. Example shape calculations for expressions [9, 16] have been performed, but the algebraic expressions in the examples are limited to those that produce combined cuboidal and octahedral Wulff shapes.

This work gives a general method of defining a function $\gamma(\hat{n})$ that can be used to describe a specific Wulff shape W, expanding the numerical method in [9], and a numerical analysis in general, to a larger class of material systems. Included are several two- and three-dimensional examples demonstrating the calculation of W with the Cahn-Hoffman capillarity vector $\vec{\xi}(\hat{n})$ [17, 18] that can be determined from a homogeneous extension of $\gamma(\hat{n})$ to all vectors, $A\gamma(\hat{n}) = \gamma(\vec{A})$, where each normal $\hat{n}$ describes interface of (the same) area A.

Although the Wulff construction [6] and a number of other constructions [19, 20] are equivalent methods of determining a Wulff shape, the capillarity vector is convenient because it traces W and can be expressed in terms of vector derivatives of $\gamma(\vec{A})$. Furthermore, $\vec{\xi}(\hat{n})$ is mathematically similar to other thermodynamic potentials, giving instructive analogies to phase diagrams [4], and is used to calculate the effect of curvature or particle size on interface chemical potential [21] and interface motion [22].

2. The convex surface tension and its relation to its Wulff shape

Every $\gamma(\hat{n})$ has a unique W, but a single W can be derived from an infinite number of $\gamma(\hat{n})$. Physical equilibria—including the computations described in [9, 12, 16]—depend only on W. This result follows from

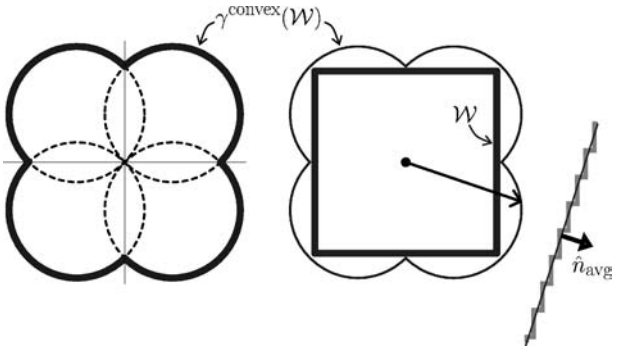

Figure 1 The convex surface tension construction builds $\gamma^{\text{convex}}(W)$ from W by intersecting spheres with the $\gamma(\hat{n})$ origin and points corresponding to the energy of facets that meet along an edge or at a corner. The outer envelope of the spheres gives $\gamma^{\text{convex}}(W)$ (top left), and $\gamma^{\text{convex}}(W)$ is the lower bound of $\gamma(W)$ that give W (top right). For interface described by $\gamma^{\text{convex}}(W)$, the energy of an orientation absent from W cannot be reduced by the local creation of steps from adjacent W interface with dimensions equal to the projection of the interface area onto the adjacent W interface. Considering only interfacial free energies, one member of an infinite set of stepped structures is shown in the figure for the fixed average orientation indicated.

the surface tension function that can be derived directly from W by equating the energy per unit projected area of any orientation (given by inclination $\hat{n}$) that does not appear on W with the sum of the energy contributions of facets that join at a corner or edge which can be combined to give the same average orientation.

This convex surface tension construction (Fig. 1) puts the energy per unit area of any (non-appearing) orientation on a sphere that has one point at the origin and is tangent to $\gamma(\hat{n})$ at any facet orientation, reproducing the *Tangent Sphere* construction of Herring [19]. The minimal surface energy density is thus defined for any polyhedral W by the outer envelope of spheres sharing the $\gamma(\hat{n})$ origin and meeting at cusps defined by the intersections of two (orthogonal to W edges) or more (at W facets) such spheres.

The minimal surface energy density is *convex* in the sense that the energy at any orientation cannot be further reduced by replacement with any other orientations which, when combined, preserve the original orientation. Interfaces that attain their convex energy with fixed average inclination as the only constraint will have no driving force to change morphology (Fig. 1). However, if the average inclination constraint is relaxed, driving forces to rotate interface into cusp orientations, *torques*, can exist, and an interface enclosing a fixed (isolated) volume will reach equilibrium by assuming the Wulff shape because W gives the smallest interfacial free energy to volume ratio.

Let the convex energy functions be called $\gamma^{\text{convex}}(W)$. Different $\gamma(\hat{n})$ that have the same W will be called *equivalent* or in *the equivalence class* $\gamma(W)$ and denoted $\gamma^W(\hat{n})$[2]. All equivalent $\gamma(\hat{n})$ must lie outside $\gamma^{\text{convex}}(W)$ except at facet orientations where they must coincide. It is necessary that any $\gamma^W(\hat{n})$ have cusps at least as "sharp" as those of $\gamma^{\text{convex}}(W)$.

For a numerical equilibrium calculation, any member of a W's equivalence class will give an identical result because the numerical method automatically "convexifies" $\gamma^W(\hat{n})$—for an interface that does not enclose a fixed volume, the method creates any average orientation $\hat{n}_{\text{avg}}$ from nearby orientations of W in proportions that map the resultant energy to the convexified surface tension $\gamma^{\text{convex}}(W)|_{\hat{n}=\hat{n}_{\text{avg}}}$.

3. The numerical minimizing $\gamma(\hat{n})$ sequence

The numerical method (*Surface Evolver* [23]) in [9] finds an energetic minimum by successive discrete iteration. It is therefore most suitable to a differentiable function, and polyhedral W present numerical difficulties because their $\gamma^W(\hat{n})$ cannot have continuous derivatives at $\hat{n}$ belonging to facets. We surmount these difficulties by using a family $\gamma(\hat{n}, \alpha)$ differentiable for all $|\alpha| < 1$ but limited by a member of a specified W's equivalence class—that is, taking $0 \leq \alpha \leq 1$ for simplicity, $\lim_{\alpha\to 1}\gamma(\hat{n}, \alpha) = \gamma^W(\hat{n})$. Thus, the method finds the minimizing shape for a non-smooth $\gamma^W(\hat{n})$ by first numerically approximating a $W(\alpha)$ with finite curvature in regions where W is flat by minimizing for a fixed, finite α and then proceeding to a crystalline shape in $W = \lim_{\alpha\to 1} W(\alpha)$.

4. Algebraic formula for an instance of $\gamma(W)$

The following sections demonstrate methods of constructing $\gamma^W(\hat{n})$ for use in a numerical analysis of equilibrium shape and microstructural evolution. To produce energetically favorable orientations, the $\gamma^W(\hat{n})$ are constructed from functions that have minima at specified inclinations. For example, a minimum could be arranged at $\hat{n}^{\text{fixed}}$ via a quadratic $(\hat{n}-\hat{n}^{\text{fixed}})\cdot(\hat{n}-\hat{n}^{\text{fixed}})$ or another function that has lowest order even terms in its Taylor expansion about a point, and a cusp-minima could be modeled with $|\pi/2 - \cos^{-1}(\hat{n}\cdot\hat{n}^{\text{fixed}})|$. However, there are many other choices, and some work better than others. The methods demonstrated below differ in how the "distance" between $\hat{n}^{\text{fixed}}$ and $\hat{n}$ is specified and subsequently penalized. Because the Wulff construction forms low-energy orientations in proportions that minimize the *total* surface energy over a fixed volume, it does not have a "local" dependence on γ—changes in γ at an inclination $\hat{n}$ with, e.g., temperature, can affect the Wulff shape at inclinations that are not in the neighborhood of $\hat{n}$.

Although a Wulff shape with a single facet surrounded by an edge isolating it from a smoothly curved (i.e., rough) portion is very artificial, it is used for the two-dimensional examples below because it provides a useful test case.

4.1. Producing minima in $\gamma(W)$ with "directional" distance

A $\gamma^W(\hat{n})$ is calculated by considering, for every direction $\hat{n}$, the distance between $\hat{n}$ and each minima weighted by the depth of the minima relative to an isotropic reference of radius γ_o[3]. When there is only one minimum, located at $\hat{n}^{\text{fixed}}$, the formulations in this section take the following form,

$$\gamma(\vec{A}, \alpha) = \gamma_o A\left[1 - \alpha\left(\frac{d_{\max} - d(\hat{n})}{d_{\max} - d_{\min}}\right)\right] = \gamma_o A[1 - \alpha D(\hat{n})] \quad (1)$$

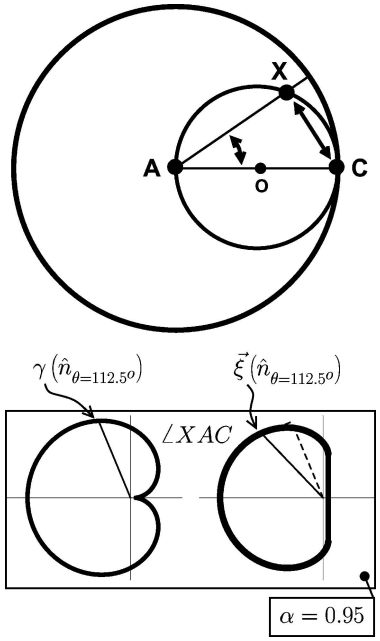

Figure 2 To create $\gamma(\hat{n})$ minima, energy is subtracted along each point X of an isotropic reference sphere, γ_o (top). This illustration uses bold double arrows to mark two metrics that are directly applicable in the creation of a $\gamma(W)$: $\angle XAC$ and $\overline{XC}$. The diameter of the γ_o-circle along $\vec{C}$ defines the radius of an embedding circle that is useful for measuring distance in the calculations. Plots of $\gamma(\hat{n})$ and $\vec{\xi}(\hat{n})$ calculated for $\alpha = 0.95$ for $d(\hat{n}) = \angle XAC$ (bottom). Note that $\vec{\xi}(\hat{n})$ is not generally parallel to $\hat{n}$.

where each orientation has an area of magnitude A, the depth of the minimum relative to γ_o is determined by the anisotropy factor α, and the distance (taken according to an as of yet unspecified metric) between point $X(\hat{n}) = \gamma_o\hat{n}$ on the γ_o-sphere and the point C^{fixed} on the sphere defined by ray $\vec{C}$ extending from the origin through the minimum is $d(\hat{n})$. Equation 1 uses the geometry in Fig. 2. Variables $d_{\max}$ and $d_{\min}$ are the maximum and minimum possible $d(\hat{n})$ values, giving $D(\hat{n}) = 1$ when $\hat{n}$ points directly toward the minimum and $D(\hat{n}) = 0$ when $\hat{n}$ points directly opposite the minimum.

Equation 1 is generally an approximation to a single-facet W. As before, $\gamma^{\text{convex}}(W)$ is defined by the outer envelope of spheres passing through the origin and adjacent minima—in this case of a non-polyhedral W, one minimum generates a broad facet and a nearby continuous set of minima generates the smoothly curved portion of W[4]. Equation 1 is an approximation if the $\gamma(\hat{n})$ do not match, exactly, the set of minima producing the curved portion of W. This is shown in Sections 4.2 and 4.3 for two $\gamma(\hat{n})$ containing a single cusp of the same inclination and depth that give different W.

When $\gamma(\hat{n}, \alpha)$ contains multiple minima, the anisotropy factor that specifies the reduction in energy must account for the proximity and depth of neighboring minima. In this case, the single distance must be replaced with a summation over all minima weighted by a factor that yields the desired reduction in energy for a fixed α

$$\gamma(\vec{A}, \alpha) = \gamma_o A\left(1 - \alpha \sum_{i=1}^{M} w_i D_i(\hat{n})\right) \qquad (2)$$

where M is the total number of minima, w_i shifts minimum i to the desired depth, $D_i(\hat{n})$ denotes $(d_{\max} - d_i(\hat{n}))/(d_{\max} - d_{\min})$, and $d_i(\hat{n})$ is the distance between $\hat{n}$ and the inclination of minimum i.

For a set of symmetry-related minima—i. e., minima of equal depth with identical arrangements of neighboring minima—w_i is a constant and a simple two-dimensional example demonstrates the utility of Equation 2. Let $\gamma(\hat{n}, \alpha)$ converge to the equivalence class of a square W with {10} facets ($M = 4$). Let $d_i(\hat{n})$ be for this example taken with the Euclidean metric, given as the length of the chord connecting general points $X(\hat{n})$ to minima orientations C_i represented on the reference sphere. For any $X(\hat{n})$ that coincides with a {10} minima orientation,

$$\gamma(A, \alpha) = \gamma_o A\left[1 - \alpha w\left(1 + \frac{2-\sqrt{2}}{2} + \frac{2-\sqrt{2}}{2} + 0\right)\right] \qquad (3)$$

and the *anisotropic limit*, defined for $\alpha = 1$, can be specified with w. Equation 3 shows that if, for instance, $X(\hat{n})$ coincides with the (10) minimum, the interfacial free energy at that minimum feels no influence from the minimum at $(\bar{1}0)$ but a slight influence from the (01) and $(0\bar{1})$ minima.

For two distinct minima occurring along $\hat{n}_1$ and $\hat{n}_2$, the expression relating w_2 to w_1 can be determined from

$$R_{12} = \frac{\gamma(\hat{n}_1, \alpha)}{\gamma(\hat{n}_2, \alpha)} \qquad (\alpha = \text{fixed}) \qquad (4)$$

where R_{12} is the magnitude of $\gamma(\hat{n}_1, \alpha)$ relative to $\gamma(\hat{n}_2, \alpha)$. Solving for w_2,

$$w_2 = \frac{w_1[1 - R_{12}D_1(n_1)] + \frac{1}{\alpha}[R_{12}(1 - S_2) - (1 - S_1)]}{[R_{12} - D_2(n_1)]} \qquad (5)$$

The S_1 and S_2 are positive constants corresponding to the remainder of the summations in $\gamma(\hat{n}_1, \alpha)$ and $\gamma(\hat{n}_2, \alpha)$ due to the presence of minima in other directions. This expression shows that it becomes increasingly difficult (w_2 must be very large) to satisfy Equation 2 both in the *isotropic limit* ($\alpha = 0$) and as the distance between the minima of $\hat{n}_1$ and $\hat{n}_2$ approaches R_{12}. The expression also shows that the value of w_2 reflects the effect of neighboring minima. If $\gamma(\hat{n}_1, \alpha) > \gamma(\hat{n}_2, \alpha)$, a smaller w_2 is needed when S_2 is large because this implies that $\hat{n}_2$ is close to very deep or several minima that reduce $\gamma(\hat{n}_2, \alpha)$. Direct control over multiple distinct sets of minima may require an iterative solution to a set of equations resulting from Equation 2 because adjusting w_i for one set of minima can affect the relative depth of all minima.

The precise shape of $\gamma(\hat{n}, \alpha)$ depends on how the distance $d(\hat{n})$ is quantified. Variations along the surface of $\gamma(\hat{n})$-plots indicate how quickly the distance changes with $\hat{n}$ according to the metric used. The

dependence on $\hat{n}$ could affect predictions on how the shape of $\gamma^W(\hat{n})$ will change with, for instance, an increase in the depth of a single set of equivalent cusps that occurs on chemical adsorption or lowering the temperature. Consequently, the behavior predicted with a surface energy model can depend sensitively on the choice of functional representation. Generally, reconstructions of observed crystalline (polyhedral) W do not require the detailed knowledge of $\gamma^W(\hat{n})$ shapes. However, exact $\gamma^W(\hat{n})$ or portions of exact $\gamma^W(\hat{n})$ are necessary for changes to W with an intensive variable giving rise to new features (facets, edges, corners) and for W that contain contiguous orientations of interface.

The next two sections use the two-dimensional $<hk0>$ example of equilibrium shapes with a single facet at (100) to demonstrate constructions of $\gamma^W(\hat{n})$ for general W. The first section uses an angular metric to assign values to $d(\hat{n})$. To demonstrate that there is more than one way to build a feasible $\gamma(\hat{n})$, the second section uses the Euclidean metric. To illustrate difficulties that may arise on forming a crystalline $\gamma(\hat{n})$, these two sections are followed by a third giving a $\gamma(\hat{n})$ that always yields isotropic shapes and a fourth giving a $\gamma(\hat{n})$ often used in the literature that is useful for W of cubic symmetry. These sections are followed with three-dimensional implementations of the methods, producing $\gamma(\hat{n})$ that give W of general symmetry, to demonstrate their practical utility.

Before the examples, we briefly outline the steps used in constructing W from a $\gamma^W(\hat{n})$ that takes distance from specified minima as a parameter:

1. Orient the directions of $\gamma(\hat{n})$ minima on a unit sphere
2. Choose a metric to describe $d(\hat{n})$, the distance between the direction of these minima and an arbitrary direction
3. Use $d(\hat{n})$ with γ_o to define a $\gamma(\hat{n})$ that is HD1 (homogeneous of degree one)[5]
4. Extend this $\gamma(\hat{n})$ to all area vectors by multiplying by A, $\gamma(\vec{A}) = A\gamma(\hat{n})$
5. Take the gradient with respect to $\vec{A} = A\hat{n}$

The capillarity vector is defined

$$\vec{\xi}(\hat{n}, \alpha) = \vec{\nabla}_{\vec{A}}[A\gamma(\hat{n}, \alpha)] \tag{6}$$

and an HD0 result from the last step is the $\xi(\hat{n}, \alpha)$, and thus the $W(\alpha)$, for the $\gamma(\hat{n}, \alpha)$ formulated.

4.2. Angular distance

Angular distances taken directly from the origin of the reference γ_o-sphere, $\angle XOC$, could be used in the construction of anisotropic $\gamma(W)$. However, $\gamma^W(\hat{n})$ derived from $\angle XOC$ through Equation 2 require further manipulation to reconstruct a given W. Reconstructions of specified W can be obtained with angular distances taken from the antipode of a minimum using radii of a sphere formed by revolving the γ_o reference sphere about the antipode, illustrated in Fig. 2 for two dimensions. Distance $d(\hat{n})$ is then taken as the angle $\angle XAC$ between radii of the larger sphere. For convenience, we will call these angular distances $\angle XAC$ distances taken with the $\angle XAC$ metric. Use of the $\angle XAC$ metric is demonstrated below by constructing an equivalent $\gamma(\hat{n})$ with a minima along $\vec{C} = [100]$.

For this example, $(d_{\min}, d_{\max}) = (0, \pi/2)$ and Equation 1 becomes

$$\gamma(\vec{A}, \alpha) = \gamma_o A\left(1 - \alpha\left\{1 - \frac{\arccos\left[\frac{1}{2}(1+n_1)\right]}{\frac{\pi}{2}}\right\}\right) \tag{7}$$

where

$$\hat{n}=(n_1, n_2, n_3) = \frac{(x\hat{i}, y\hat{j}, z\hat{k})}{\sqrt{x^2+y^2+z^2}} \quad (A=\|\vec{A}\cdot\hat{n}\|) \tag{8}$$

the center of the γ_o-sphere remains the origin of the reference coordinate system, and the 1/2 in the argument of the arccos corresponds to the $2\gamma_o$-radius. As in the following two-dimensional examples, $\alpha = 0$ reverts to a sphere, and larger values of α produce minima along $\hat{n}_{[100]}$ with $\gamma(\hat{n}_{[100]}) \to 0$ in the anisotropic limit.

The $\vec{\xi}(\hat{n}, \alpha)$ calculated from Equation 7 is

$$\begin{aligned}
\vec{\xi}(\hat{n}, \alpha) &= (\xi_1, \xi_2, \xi_3) \\
\xi_1 &= \frac{\alpha\left(n_1^2 - 1\right)}{\pi\sqrt{1 - \frac{1}{4}(1+n_1)^2}} + n_1\frac{\gamma(\vec{A}, \alpha)}{\gamma_o A} \\
\xi_2 &= \frac{\alpha n_1 n_2}{\pi\sqrt{1 - \frac{1}{4}(1+n_1)^2}} + n_1\frac{\gamma(\vec{A}, \alpha)}{\gamma_o A} \\
\xi_3 &= 0
\end{aligned} \tag{9}$$

The plot of $\vec{\xi}(\hat{n}, \alpha)$ in Fig. 2 shows that the $\angle XAC$ metric produces the (100) facet designated through Equation 7. The capillarity vector can be decomposed into two parts. In the anisotropic limit, $\vec{\xi}(\hat{n}) = \gamma(\hat{n})\hat{n} + \vec{\xi}_\tau(\hat{n})$, where $\gamma(\hat{n})\hat{n}$ acts along n and indicates the ability to decrease free energy by eliminating interface area, and $\vec{\xi}_\tau(\hat{n})$ (the torque per unit interface area) acts perpendicular to $\hat{n}$ and indicates the ability to decrease free energy by rotating $\hat{n}$ [17, 24]. Plotting $\vec{\xi}_\tau(\hat{n})$ for all inclinations shows the torque to continuously decrease to zero as $\hat{n}$ moves from the [100] cusp to the cusp antipode ($[\bar{1}00]$)—i.e., this model $\gamma(\hat{n})$ gives torques acting to rotate interface into the cusp orientation that are greatest near the cusp, where they assume a limiting value of $\sqrt{2}/\pi$.

4.3. Chord distance

The Euclidean metric, giving the length of the chord connecting $X(\hat{n})$ and C on the γ_o-sphere, provides a simple route to results nearly identical to the $\angle XAC$ metric. For convenience, we will call the length $\overline{XC}$ determined by the Euclidean metric distance taken with the $\overline{XC}$ metric. The $\overline{XC}$ metric always places a point on the γ_o-sphere further from the cusp than $\angle XAC$. As a result, $\overline{XC}$ assigns larger values to orientations off of the minima.

A standard way of measuring the difference between two shapes is taking the symmetric difference between them

$$W_{\angle XAC} \Delta W_{\overline{XC}} \tag{10}$$

which is the union of the portion of $W_{\angle XAC}$ that lies outside of $W_{\overline{XC}}$ with the portion of $W_{\overline{XC}}$ that lies outside of $W_{\angle XAC}$. The number of elements in the set represented by Equation 10 diminish as the shapes converge, and a null set is produced when the shapes are identical [25]. The symmetric difference of Equation 10 is visibly small with respect to the volume of the shapes calculated above for a single facet, and crystalline $\gamma(\vec{A})$– and $\vec{\xi}(\hat{n})$ -plots produced by $\angle XAC$ and $\overline{XC}$ metrics are essentially identical at a given α.

Using the $\overline{XC}$ metric gives

$$\gamma(\vec{A}, \alpha) = \gamma_o A\left[1 - \alpha\left(1 - \frac{1}{2}\sqrt{(n_1 - 1)^2 + n_2^2}\right)\right] \tag{11}$$

for a [100] cusp and the equation for $\vec{\xi}(\hat{n}, \alpha)$ that follows is in the Appendix. From a practical standpoint, the numerical evaluation of the $\gamma(\hat{n}, \alpha)$ and $\vec{\xi}(\hat{n}, \alpha)$ that derive from an $\overline{XC}$ metric require less time than those from $\angle XAC$. For calculations at the same fixed α, formulations based on the $\overline{XC}$ metric typically reduce computing time by 25–50%.

4.4. Projections of chord distances on diameter through cusp

As a logical extension of results from the previous section, one might postulate that projections of $\overline{XC}$ onto the diameter of the γ_o-sphere along $\vec{C}$ would provide a convenient metric that builds plots of $\gamma(\hat{n})$ and $\vec{\xi}(\hat{n})$ comparable to those of the $\overline{XC}$ and $\angle XAC$ metrics. The metric would be convenient because it yields a relatively simple formulation

$$\gamma(\vec{A}, \alpha) = \gamma_o A\left[1 - \frac{\alpha}{2}(n_1 + 1)\right] \tag{12}$$

The addition of one to n_1 accounts for the location of the antipode, which is at point $(-\gamma_o, 0)$, and the division by two appears because projections are on the full length of the diameter. Equation 12 uses the length of the diameter that is not projected, i.e., $\overline{AP} = 2\gamma_o - \overline{PC}$, where $\overline{AC}$ is γ_o-sphere diameter through the cusp and P is the interior terminus of the projection, to reveal the geometry.

The $\overline{AP}$ metric creates a $\gamma(\hat{n})$-plot with a minimum that, relative to that produced by of $\angle XAC$ and $\overline{XC}$, is shallow because a larger neighborhood of points adjacent to the minimum are influenced by its depth. The $\vec{\xi}(\hat{n}, \alpha)$ calculated from Equation 12 is not anisotropic—i.e., $\vec{\xi}(\hat{n}, \alpha)$ always traces a circle in two dimensions and a sphere in three dimensions. The center of the circle does not share the common origin of the $\gamma(\hat{n}, \alpha)$– and $\vec{\xi}(\hat{n}, \alpha)$–plots but is displaced toward the cusp antipode as in Fig. 2. In effect, $\vec{\xi}(\hat{n}, \alpha)$ is the parametric equation of a circle with a radius of $\gamma_o(1 - \alpha/2)$ that is centered at $(-\alpha/2, 0)$, and it is not useful for creating general Wulff shapes.

4.5. Convenient methods for shapes of cubic symmetry

A formulation for $\gamma(\hat{n})$ often employed to create W in various microstructural models [9, 16] is

$$\gamma(\vec{A}, \alpha) = \gamma_o A\left[1 - \alpha\left(1 - n_1^2 n_2^2 + n_3^2 n_1^2 + n_2^2 n_3^2\right)\right] \tag{13}$$

The form derives from expressions that are invariant to cubic symmetry operations on $n1, n2, n3$ [16].

The following exercise demonstrates why cubic symmetries are always produced for $\alpha \neq 0$. When Equation 13 is evaluated for $\hat{n}$ parallel to the [100]-axis, two of $(n1, n2, n3)$ are zero, and $\gamma(\vec{A}, \alpha) = \gamma_o A$. As $\hat{n}$ rotates clockwise from this axis to trace the locus of points defining a unit circle in the $(hk0)$ plane, $\gamma(\vec{A}, \alpha)$ decreases from a maximum of $\gamma_o A$ for (100) interface to a minimum of $\gamma_o A(1 - \alpha/4)$ for $(1\bar{1}0)$ interface. On completing the circle, $\hat{n}$ has taken $\gamma(\vec{A}, \alpha)$ through four maxima and four minima that are related through a four-fold axis of symmetry passing through the origin and parallel to [001]. Consequently, a positive value of a will produce local minima at {110} orientations that give way to four facets in the $\vec{\xi}(\hat{n}, \alpha)$ plot on increasing α.

Unstable orientations appear in this example along <110>, halfway between two facets, for $\alpha \geq 4/11$. Although W is traced by $\vec{\xi}(\hat{n})$, the two are not always identical because W is an equilibrium shape and therefore does not contain unstable orientations that are marked by regions of multivalued $\vec{\xi}(\hat{n})$. As a result, W replaces spinodal portions of $\vec{\xi}(\hat{n})$ with corners and edges to—for the anisotropic limit in this example—create a square in the $(hk0)$ plane.

5. Three-dimensional examples

The previous sections demonstrate that multiple methods can be used to generate a $\gamma^W(\hat{n})$.

Below, the utility of these $\gamma(\hat{n})$ is briefly demonstrated through three-dimensional examples obtained with a simple extension of the two-dimensional formulations. The first example calculates $\gamma(\hat{n})$ for eight symmetrically equivalent {111} minima with both metrics to verify their near equivalence in three dimensions, and the remaining examples generate shapes under the $\overline{XC}$ metric only.

5.1. Eight equivalent <111> minima

To calculate a W with eight identical {111} facets, the general form of $\gamma(\vec{A}, \alpha)$ is

$$\gamma(\vec{A}, \alpha) = \gamma_o A\left\{1 - \alpha w\left[8 - \frac{\sqrt{2}}{2}\left(\sum_{i=1}^{2}\sum_{j=0}^{1}\sum_{k=1}^{2} \times \sqrt{1 + \frac{(-1)^i n_1 + (-1)^j n_2 + (-1)^k n_3}{\sqrt{3}}}\right)\right]\right\} \tag{14}$$

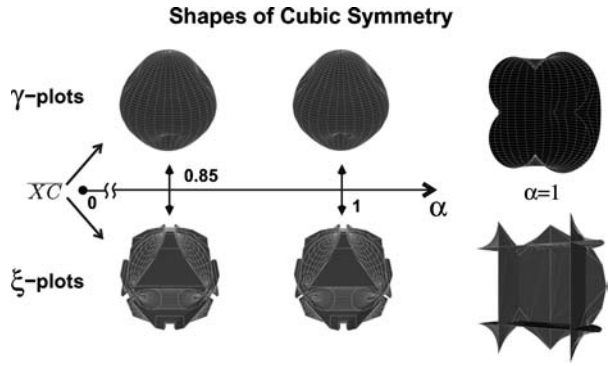

Figure 3 Three-dimensional $\gamma(\hat{n})$ and $\vec{\xi}(\hat{n})$ calculated using $\overline{XC}$ metric. (Left) shows $\gamma(\hat{n})$ belonging to an equivalence class of an octahedron W for two values of α. (Right) shows half of the three-dimensional plots for $\gamma(\hat{n})$ belonging to a cube W. Because the $\gamma(W)$ are not convex, spinodal portions, replaced with W by edges and corners, occur in the $\vec{\xi}(\hat{n})$-plots.

for the $\overline{XC}$ metric and

$$\gamma(\vec{A},\alpha)=\gamma_o A\left\{1-\alpha w\left[8-\frac{2}{\pi}\sum_{i=1}^{2}\sum_{j=0}^{1}\sum_{k=1}^{2}\left(\arccos\frac{1}{2}+\frac{(-1)^i n_1+(-1)^j n_2+(-1)^k n_3}{2\sqrt{3}}\right)\right]\right\} \quad (15)$$

for the $\angle XAC$ metric.

Three-dimensional $\gamma(\hat{n})$- and $\vec{\xi}(\hat{n})$-plots calculated from Equation 14 are shown in Fig. 3. In each case, w was calculated so that $\gamma(\hat{n}_{(111)}) \rightarrow 1/8$ as $\alpha \rightarrow 1$ to define a shape with finite surface energy in the anisotropic limit. For Equation 14, this gives $w \approx 0.25$, and $w \approx 0.31$ for Equation 15.

Similar to results from the two-dimensional calculations, the $\overline{XC}$ and $\angle XAC$ metrics converge to essentially the same W in the anisotropic limit. Further analysis shows the $\overline{XC}$ metric to yield slightly more compact shapes at a given value of a for which non-crystalline shapes are calculated. Because crystalline shapes can be considered identical, the following examples use only the $\overline{XC}$ metric.

5.2. Six equivalent <100> minima

For this example, six {100} facets are produced from the following equation

$$\gamma(\vec{A},\alpha)=\gamma_o A\left(1-\alpha w\left\{6-\frac{\sqrt{2}}{2}\times\left[\sum_{i=1}^{3}\sum_{j=1}^{2}\left(\sqrt{1+(-1)^j n_i}\right)\right]\right\}\right) \quad (16)$$

where $w \approx 0.40$ was calculated as in the previous section.

Fig. 3 shows one set of $\gamma(\hat{n})$- and $\vec{\xi}(\hat{n})$-plots corresponding to the half located beneath the $(hk0)$ plane to illustrate the perhaps more conventional two-dimensional projections of the plots.

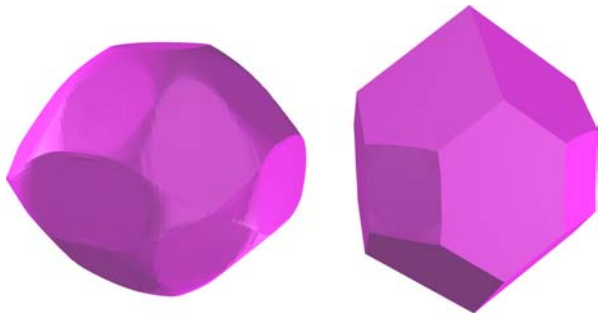

Figure 4 Shapes of general symmetry obtained with the $\angle XAC$ metric. The example belonging to W^{general} (left) has 18 minima, 8 of which are along $<1\sqrt{2}\sqrt{3}>$, 6 along $<\sqrt{3}10>$, and 4 along $<101>$. The tetrahedral $\gamma(W^{\text{tetrah}})$ (right) has a rutile-like form, with 12 $<110>$ minima and 4 $<100>$ minima.

5.3. Minima of various symmetry

Fig. 4 gives two crystalline $\{\gamma(\hat{n}), \vec{\xi}(\hat{n})\}$ examples of different symmetry: a tetragonal shape defined by twelve {110} and four {100} facets with a 4-fold rotation axis along $<001>$, and a general shape defined by eight $\{1\sqrt{2}\sqrt{3}\}$, six $\{\sqrt{3}10\}$, and four {101} facets with 2-fold rotation axis along $<001>$. The equations for these shapes are not written explicitly but can be derived with the methods demonstrated.

6. Summary

The Wulff shape determined experimentally for any particle can be used to construct the convexified $\gamma^{\text{convex}}(W)$ that holds for the particle under the conditions of the observation. Useful calculations of changes in interface structure to achieve equilibrium or under external driving forces result with $\gamma(\hat{n})$ in the equivalence class to W that can be obtained from $\gamma^{\text{convex}}(W)$.

Two-dimensional examples of a particle with a single facet demonstrate the construction of $\gamma(W)$ suitable for shape calculations. The examples use both angular ($\angle XAC$) and Euclidean ($\overline{XC}$) distance between directions $\hat{n}$ oriented on a reference γ_o-sphere to make $\gamma^W(\hat{n})$ for equilibrium shapes with a (100) facet. It is also shown that, although the mathematical restrictions on $\gamma(\hat{n})$ and $\vec{\xi}(\hat{n})$ may be satisfied, not all metrics produce formulations of $\gamma(\hat{n})$ that give the correct W. Working $\gamma^W(\hat{n})$ that belong to the same equivalence class converge to the same W if $\gamma^{\text{convex}}(W)$ is crystalline but can otherwise have a small but finite symmetric difference, where $W_1 \Delta W_2$ is not a null set. Further examples demonstrate how the methods can be extended to produce shapes of arbitrary symmetry in three dimensions.

The results of this work thus provide information—mathematical formulations creating equilibrium interface—that can be applied in models based on the minimization of anisotropic interfacial free energies. Currently, the results for $\gamma(W)$ are being implemented to extend the calculations of complex equilibrium shapes of [9] to all crystalline symmetries.

Appendix

Formulations for $\vec{\xi}(\hat{n}) = (\xi_1\xi_2\xi_3)$

To better understand the $\vec{\xi}(\hat{n})$-plots, the $\vec{\xi}(\hat{n})$ is dissembled below into the normal component and off-normal

(torque) components. Both vectors have n_1, n_2 and n_3 components. In each of the two-dimensional examples below, n_3 components are zero and $\vec{\xi}_n(\hat{n})$ takes the following form

$$\begin{aligned}\vec{\xi}_n(\hat{n}) &= \left(\vec{\xi}_{n_1}(\hat{n}), \vec{\xi}_{n_2}(\hat{n}), 0\right) \\ &= \left(\frac{\gamma(\hat{n})}{\gamma_o} n_1, \frac{\gamma(\hat{n})}{\gamma_o} n_2, 0\right)\end{aligned} \tag{17}$$

Ihord distance on unit γ_o sphere

$$\begin{aligned}\gamma(\hat{n}, \alpha) &= \gamma_o\left[1 - \alpha\left(1 - \frac{1}{2}B\right)\right] \\ \vec{\xi}_\tau(\hat{n}, \alpha) &= \left(-\frac{\alpha}{2}\left(n_1 B - \frac{n_1 - 1}{B}\right),\right. \\ &\quad \left. -\frac{\alpha}{2}\left(n_2 B - \frac{n_2}{B}\right), 0\right) \\ B &= \sqrt{(n_1 - 1)^2 + n_2^2}\end{aligned} \tag{18}$$

Projection of unit γ_o sphere chord onto diameter

$$\begin{aligned}\gamma(\hat{n}, \alpha) &= \gamma_o\left[1 - \frac{\alpha}{2}(1 + n_1)\right] \\ \vec{\xi}_\tau(\hat{n}, \alpha) &= \left(-\frac{\alpha}{2}\left(1 - n_1^2\right), \frac{\alpha n_1 n_2}{2}, 0\right)\end{aligned} \tag{19}$$

Method for cubic symmetry

$$\begin{aligned}\gamma(\hat{n}, \alpha) &= \gamma_o\left[1 - \alpha\left(1 - n_1^2 n_2^2 + n_3^2 n_1^2 + n_2^2 n_3^2\right)\right] \\ \vec{\xi}_\tau(\hat{n}, \alpha) &= \left(-2\alpha\left[2n_1^3\left(n_2^2 + n_3^2\right) - n_1\left(n_2^2 + n_3^2\right)\right],\right. \\ &\quad \left. -2\alpha\left[2n_2^3\left(n_3^2 + n_1^2\right) - n_2\left(n_3^2 + n_1^2\right)\right], 0\right)\end{aligned} \tag{20}$$

References

1. J. W. CAHN, in "Segregation to Interfaces," edited by W.C. Johnson and J.M. Blokely (Am. Soc. Metals Press, Metals Park, OH, 1979), p. 3.
2. J. W. CAHN, *J. de Physique* **43**(12) (1982) 199.
3. L. KAUFMAN and H. BERNSTEIN, "Computer Calculations of Phase Diagrams" (Academic Press, New York, 1970).
4. J. W. CAHN and W. C. CARTER, *Metall. Mater. Trans. A* **27**(6) (1996) 1431.
5. I. FONSECA and S. MIDLER, *Proc. Roy. Soc. of Edin., A-Mathem.* **119**(1–2) (1991) 125.
6. G. WULFF, *Z. Krist. Mineral* **34** (1901) 449.
7. Jean E. Taylor, *Bull. AMS* **84** (1978) 568.
8. R. K. P. ZIA, *Physica A* **251**(1–2) (1998) 40.
9. E. J. SIEM, W. C. CARTER and D. CHATAIN, *Phil. Mag.* **84**(10) (2004) 991.
10. J. K. LEE and H. I. AARONSON, *Acta Metall.* **23** (1975) 799.
11. *Idem., ibid.* **23** (1975) 809.
12. E. J. SIEM, Ph.D. Thesis, M.I.T. (unpublished).
13. C. S. SMITH (quoting C. Zener), *Trans. Metall. Soc. A.I.M.E.* **175** (1948) 15.
14. C. H. HSUEH, A. G. EVANS and R. L. COBLE, *Acta Metall. Mater.* **30**(7) (1982) 1269.
15. G. GOTTSTEIN and L. S. SHVINDLERMAN, *ibid.* **41** (1993) 3267.
16. W. C. CARTER and C. A. HANDWERKER, *Acta Metall. et Mater.* **41**(5) (1993) 1633.
17. D. W. HOFFMAN and J. W. CAHN, *Surf. Sci.* **31** (1972) 368.
18. J. W. CAHN and D. W. HOFFMAN, *Acta Met.* **22** (1974) 1205.
19. C. HERRING, *Phys. Rev.* **82**(1) 87 (1951).
20. F. C. FRANK, "in Metal Surfaces, Structure, Energetics, and Kinetics," (Am. Soc. Metals, Cleveland, OH, 1963), p. 1.
21. J. E. TAYLOR, *Acta Metall. Mater.* **40** (1992) 1475.
22. W. CRAIG CARTER, J. E. TAYLOR and J. W. CAHN, *JOM* **49**(12) (1997) 30.
23. K. A. BRAKKE, "The Surface Evolver," 1990 http://www.susqu.edu/facstaff/b/brakke/evolver/, Source code and manual freely available.
24. C. HERRING, in "The Physics of Powder Metallurgy," edited by W.E. Kingston (McGraw-Hill, New York, 1951), p. 143.
25. F. ALMGREN and J. E. TAYLOR, *Fractals* **3** (1995) 3713.

Received 16 September 2004
and accepted 31 January 2005